Journal of Applied Science and Engineering, Vol. 22, No. 2, pp. 239–248 (2019) DOI: 10.6180/jase.201906_22(2).0005

Development of an Ultrasonic Drilling Machine with Portability

Hongbing Wang[1,2]* and Chunhua Sun[1,2]

[1]Department of Mechanical & Electrical Engineering, Suzhou Vocational University, Suzhou 215104, P.R. China
[2]3C-Product Intelligent Manufacturing Engineering Technology Research and Development Center, Suzhou 215104, P.R. China

Abstract

A portable effective ultrasonic drilling equipment was designed and fabricated to drill holes of hard and crisp materials such as dirt, ceramic tile, limestone, granite, basalt, sandstone and glass. The equipment included an ultrasonic generator, an ultrasonic vibrator and a tool part. Through finite element sensitivity analysis and optimization, the ultrasonic vibrator had proper first longitudinal mode frequency and larger amplitude ratio. After optimization, the first order longitudinal mode frequency was changed from 20.35 to 21.63 kHz and the ratio was changed from 60.1 to 186.8. Through modal test, distribution of the velocity along the axial direction of the vibrator was gotten when the vibrator was applied by the exciting signal at 80 Vp-p and 21.45 kHz. The test results indicated that the velocity of the vibrator's tip was the maximum, reached about 580 mm/s and the velocity of the vibrator's end was about 0, and the ultrasonic vibrator had larger amplitude ratio. The modal results were accorded with the finite element analysis. Seven hard and crisp materials were selected to drill holes using the equipment. The drilling experiment demonstrated that the rate of drilling Diorite was about 28.26 mm^3/min with emery mixed with water used as the working abrasive. The analysis and experiment indicated the equipment had the advantages of fast processing speed, stable performance, small volume and portability.

Key Words: Ultrasonic Drilling, Vibrator, Amplitude Ratio, Sensitivity Analysis, Optimization

1. Introduction

Ultrasonic drilling was a mechanical machining method that removed materials by brittle fracture. Under the method, abrasives were provided between the tool and workpiece. The tip of the tool vibrated in the ultrasonic frequency range. The pulse impact force caused fractures on the surface of the workpiece on the micron level. Although ultrasonic drilling was an unconventional process with low material removal rate, its application was not limited by electrical or chemical characteristics of materials of the workpiece. Above all it could be applied to drilling high-hardness materials like titanium carbide and brittle materials such as ceramics [1,2].

Ultrasonic drilling was a non traditional machining method which had insurmountable superiority comparing with conventional drilling. From the presented articles, the main problems of ultrasonic drilling devices were complex process and large volume [3–6]. It was inconvenient for personal use and carrying. At present small and portable ultrasonic drilling devices had not been explored and adopted. So the paper designed a portable ultrasonic drilling equipment which could be exploited for convenience. The equipment was adapted for machining hard brittle materials such as diorite, ceramic tile, limestone, granite, basalt, sandstone and glass. Especiallyona it was appropriate for family persl use and mobile work of individual workshop. The core part of

*Corresponding author. E-mail: whb45@163.com

the ultrasonic device was an ultrasonic vibrator. The vibrator had the most influence on the efficiency of the ultrasonic drilling equipment [7,8]. It was very important to design an effective ultrasonic vibrator.

Firstly, the ultrasonic drilling equipment was proposed. Secondly, the finite element sensitivity analysis and optimization were therefore proposed to design the ultrasonic vibrator. Base on the theoretical analysis the ultrasonic vibrator was then fabricated and assembled. Impedance, phase analysis and modal test were implemented in the ultrasonic vibrator. Seven hard and brittle materials, including direct, ceramic tile, limestone, granite, basalt, sandstone and glass were further selected for drilling experiment using the equipment. The analysis and experiment results were finally compared to reach a conclusion that the equipment had the advantages of fast processing speed, stable performance, small volume and portability.

2. Structure and Principle of the Ultrasonic Drilling Equipment

The structure of the ultrasonic drilling equipment was shown in Figure 1. The equipment was composed of a bracket, a nut, a spring, an ultrasonic vibrator, a fixed disk and a working station.

The bracket was used to support the ultrasonic vibrator which was fixed on the fixed disk through the bolts. The fixed disk and the spring were mounted on the column of the bracket through the nut. The nut was set to compress the spring. Thus the tip of the ultrasonic vibrator was pressed on the workpiece fixed on the workstation and definite pressure was generated. The ultrasonic vibrator was connected with an ultrasonic generator (not shown in Figure 1). The harmonic excitation signal which was generated from the ultrasonic generator was applied on the ultrasonic vibrator. The ultrasonic vibrator caused ultrasonic vibration and drilled holes in the workpiece.

The structure of the ultrasonic vibrator was shown in Figure 2, mainly including a counterweight block 1, a counterweight block 2, a piezoelectric ceramic, a connecting disk, a cone and a tool rod. The counterweight block 1 and 2 was used for fixing the piezoelectric ceramic and could adjust the natural frequency of the ultrasonic vibrator.

The piezoelectric ceramic was composed of many ceramic disks. The polarization and layout of the piezoelectric ceramic were shown in Figure 3. The polarization direction was expressed with "+" and "-". The ceramic disks were arranged oppositely, thus extended and shrank at the same time. When the harmonic excitation signal generated from the ultrasonic generator was applied to the piezoelectric ceramic, and the direction of the electric field applied to the ceramic was accorded with the direction of the polarization, the ceramic extended. On the contrary, the ceramic shrank [9]. The connecting disk was utilized to fix the vibrator on the fixed disk. The shape of the tool rod was a ladder shape which

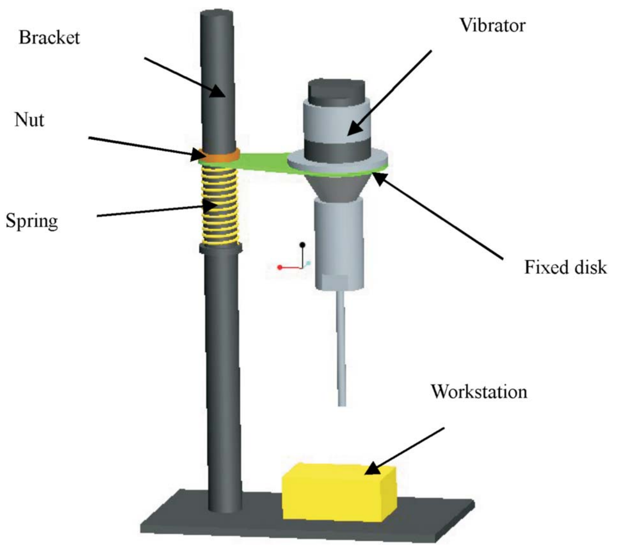

Figure 1. The ultrasonic drilling equipment.

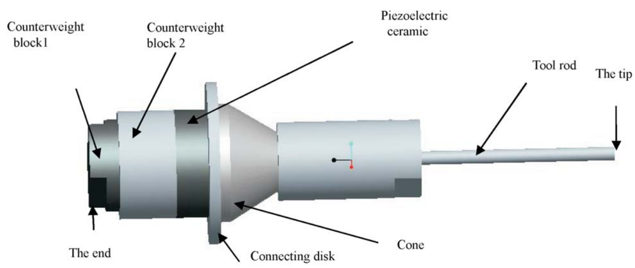

Figure 2. The ultrasonic vibrator.

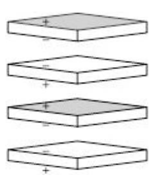

Figure 3. The polarization of the ceramic.

could amplify the vibration amplitude of the ultrasonic vibrator on the tip.While the piezoelectric ceramic extended and shrank, the tool rod was also moving along the polarization direction to drill a hole.

3. Design the Ultrasonic Vibrator by FEM Analysis

3.1 The Design Requirements of the Ultrasonic Vibrator

The first order longitudinal mode of the ultrasonic vibrator was the working mode whose frequency was accorded with the harmonic signal frequency generated by the ultrasonic generator. The harmonic signal was applied on the ultrasonic vibrator to make the ultrasonic vibrator resonate. Thus the ultrasonic vibrator caused ultrasonic vibration to accomplish drilling holes. Therefore, the ultrasonic vibrator should meet the following conditions:

(1) The ultrasonic vibrator should have proper first order longitudinal mode frequency. The drilling process could reduce noise when the working frequency was in the ultrasonic range. Simultaneously, the ultrasonic vibrator could crush the drilled materials with ultrasonic vibration. The working frequency should be above 20 kHz. However, the working frequency should not be too high, because the vibration with too high working frequency caused the piezoelectric ceramic internal loss.

(2) As showed in Figure 2, the tip of the ultrasonic vibrator crushed the workpiece directly, the tip of the vibrator should have larger vibration amplitude and the end of the ultrasonic should have small vibration amplitude. Thus, the vibration energy of the piezoelectric ceramic could be effectively passed to the tip of the ultrasonic vibrator.

(3) The ultrasonic vibrator was fixed on the fixed disk. In order to reduce the useless energy to transfer into the fixed disk, the connecting disk should be placed on the first order longitudinal node plane of the ultrasonic vibrator. The method could make the displacement of the connecting disk be minimum.

(4) The piezoelectric ceramic should be mounted on the position of maximum strain. Thus, the ultrasonic vibration energy of the piezoelectric ceramic could maximally be transferred to the tip of the ultrasonic vibrator. The piezoelectric ceramic should be placed at the first order longitudinal node plane of the ultrasonic vibrator.

3.2 The Finite Element Model of the Ultrasonic Vibrator

To meet the above conditions, the finite element model of the ultrasonic vibrator was designed by ANSYS software and shown in Figure 4. PZT-8 was selected as the material of the piezoelectric ceramic whose material parameters were shown in Table 1. Other parts of the ultrasonic vibrator were selected as 45 steel whose material properties were shown in Table 2. In the finite ele-

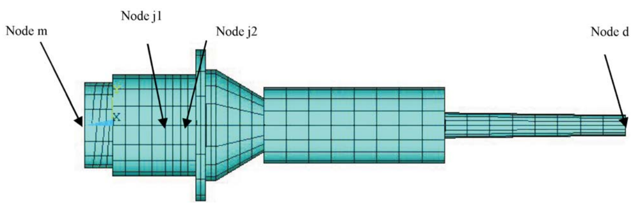

Figure 4. The finite element model of the ultrasonic vibrator.

Table 1. The material parameters of PZT-8

Parameter	Value
Dielectric constant moment [ε^T] (10^{-9} F/m)	$\begin{bmatrix} 7.124 & & \\ & 7.124 & \\ & & 5.841 \end{bmatrix}$
Piezoelectric constant matrix |d| (10^{-10} C/m^2)	$\begin{bmatrix} 0 & 0 & 0 & 0 & 10.5 & 0 \\ 0 & 0 & 0 & 10.5 & 0 & 0 \\ -4.1 & -4.1 & 14.1 & 0 & 0 & 0 \end{bmatrix}$
Stiffness matrix [c] (10^{10} Pa)	$\begin{bmatrix} 13.2 & 7.1 & 7.3 & 0 & 0 & 0 \\ & 13.2 & 7.3 & 0 & 0 & 0 \\ & & 11.5 & 0 & 0 & 0 \\ & & & 3 & 0 & 0 \\ & & & & 2.6 & 0 \\ & & & & & 2.6 \end{bmatrix}$

Table 2. The material parameters of 45 steel

Parameter	Value
Density (10^3 kg/m^3)	7.8
Elastic modulus 10^9 N/m^2)	209
Poisson ratio	0.267

ment model, solid 5 element was used to mesh the piezoelectric ceramic and solid 45 element was used to mesh the other parts of the ultrasonic vibrator.

The structure parameters of the ultrasonic vibrator were shown in Figure 5.

In Figure 5, L_1 and Φ_1 expressed respectively the length and diameter of the counterweight block 1. L_2 and Φ_2 expressed respectively the length and diameter of the counterweight block 2. L_3 and Φ_3 expressed respectively the length and diameter of the connecting disk. L_4 expressed the length of the cone block. Φ_4 expressed the bottom circle diameter of the cone. L_5 and Φ_5 expressed respectively the length and diameter of the big part of the tool rod. L_6 and Φ_6 expressed respectively the length and diameter of the small part of the tool rod.

Modal analysis of the ultrasonic vibrator was performed by using ANSYS software. The working extending and shrinking mode of the ultrasonic vibrator was the first order longitudinal mode shown in Figure 6.

Through modal analysis, the axial displacement cloud chart of the first order longitudinal mode was shown in Figure 7. The first order longitudinal mode frequency of the ultrasonic vibrator with initial structure parameters was about 20.35 kHz and the value of the axial amplitude ratio between the tip part and the end part of the ultrasonic vibrator was about 60.1. The axial amplitude ratio could be abbreviated as the ratio which was expressed in equation (1):

$$R = A_t / A_e \tag{1}$$

where R was the value of the ratio, A_t was the amplitude value of the tip part of the ultrasonic and A_e was the amplitude value of the end part of the ultrasonic.

3.3 Sensitivity Analysis

To meet the design requirements of the ultrasonic vibrator, the effects of the structure parameters on the first longitudinal mode frequency and the ratio were studied using the finite element sensitivity analysis.

Because of too many structure parameters, it was not necessary to list all parameters. Φ_5 would be selected to analyze the effect on the first longitudinal mode frequency and the ratio. Figure 8 and Figure 9 respectively expressed the effect of Φ_5 on the first longitudinal mode frequency and the ratio. From the above figures, the first longitudinal mode frequency decreased with increasing the value of Φ_5, while the ratio increased with increasing the value of Φ_5.

The sensitivity of the first order longitudinal frequency and the ratio on the structure parameters were ana-

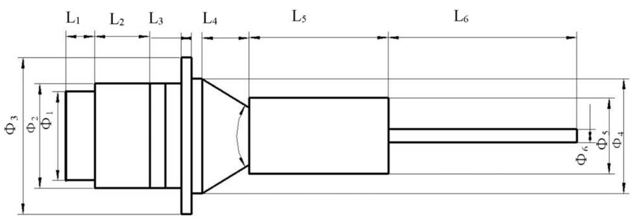

Figure 5. The structure parameters of the ultrasonic vibrator.

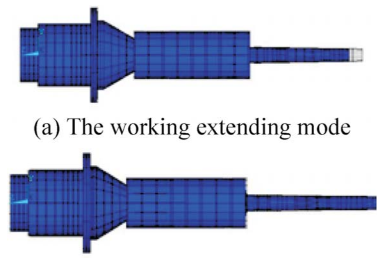

(a) The working extending mode

(b) The working shrinking mode

Figure 6. The first order longitudinal mode.

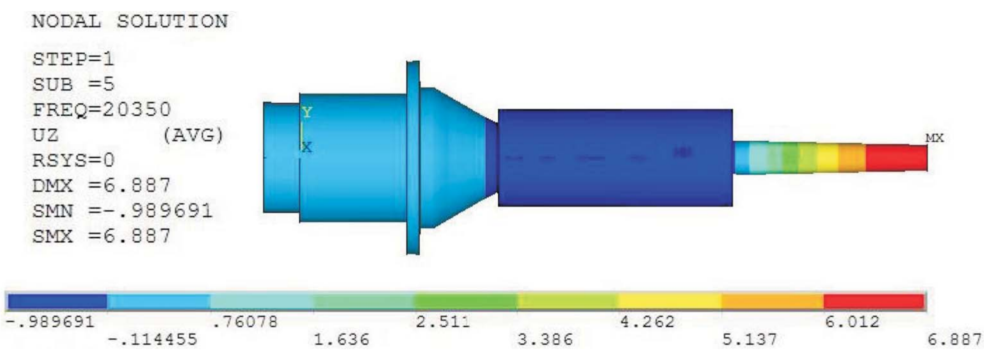

Figure 7. The axial displacement cloud chart of the first order longitudinal mode.

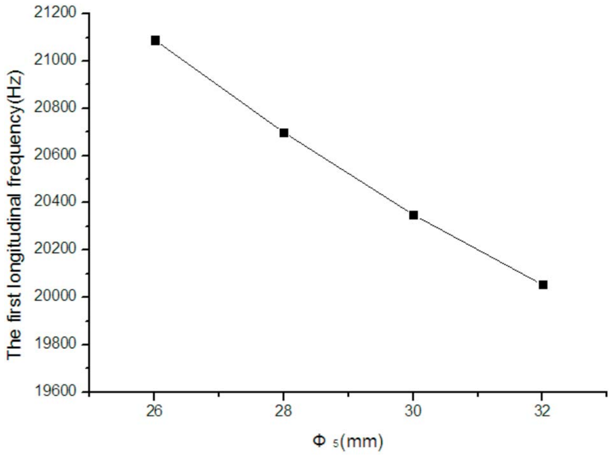

Figure 8. The effect of Φ_5 on the first longitudinal mode frequency.

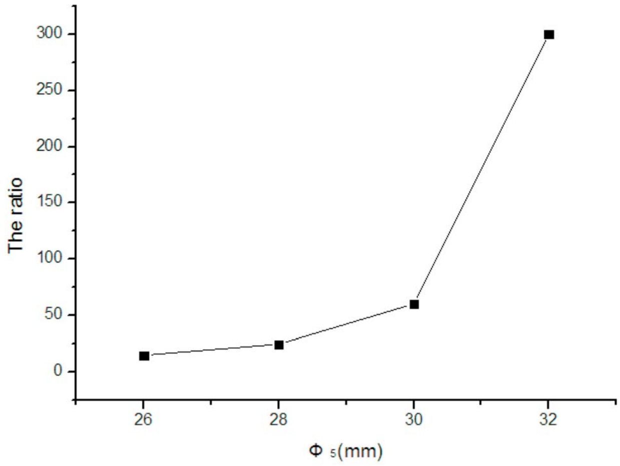

Figure 9. The effect of Φ_5 on the ratio.

lyzed by the finite element method. Thus, the structure parameters which had larger sensitivity values were selected for optimization.

The first order longitudinal frequency was expressed as ω_1 and the design variable of the structure parameter was expressed as p_j, So S_{pj} was defined as the following:

$$S_{pj} = \frac{\partial \omega_1}{\partial p_j}, j = 1, 2, \cdots, N \tag{2}$$

Here, S_{pj} was the sensitivity of the first order longitudinal frequency ω_1 on the design variable j.

The characteristic equation of the ultrasonic vibrator was expressed as the following formula.

$$K\phi_i - \omega^2 M\phi_i = 0 \ (i = 1, 2, 3, \ldots) \tag{3}$$

Here, K was the total stiffness matrix, M was the total mass matrix and ϕ_i was the i order eigen vector.

According to equation (3), equation (2) was then expressed as the following.

$$S_{pj} = \frac{\partial \omega_1}{\partial p_j} = \frac{1}{2\omega_1} \phi_1^T \left[\frac{\partial K}{\partial p_j} - \omega_1^2 \frac{\partial M}{\partial p_j} \right] \phi_1 \tag{4}$$

By using finite element method, the finite difference took the place of the partial differential. The perturbation method was used to solve equation (4). In equation (4) $\Delta p_j = 2$ mm was applied on the initial structure parameter. The sensitivity of the first order longitudinal frequency on the structure parameters were shown in Figure 10. The structure parameters of L_1, L_2, L_3, L_4, L_5, L_6, Φ_1, Φ_2, Φ_3, Φ_4, Φ_5, Φ_6 were correspondingly numbered as 1, 2, ……, 12.

In Figure 10, the numbers 5, 6, 11, 12 had greater values of the sensitivity. That meant that the structure parameters of L_5, L_6, Φ_5, Φ_6 had great influence on sensitivity.

The sensitivity of the ratio on the structure parameter was shown in Figure 11. The numbers 11, 12 had greater values of the sensitivity which respectively expressed the structure parameters of Φ_5, Φ_6.

Through the sensitivity analysis, it could be found that the structure parameters of L_5, L_6, Φ_5, Φ_6 took more affection on the first order longitudinal frequency and the ratio than the others. So the structure parameters of L_5, L_6, Φ_5, Φ_6 would be selected to optimize the first order longitudinal frequency and the ratio. The parameters values were set to change by 3 mm up and down.

3.4 Optimization Analysis of the Ultrasonic Vibrator

According to the design requirements of the ultrasonic vibrator and the sensitivity analysis, the optimization model was established.

(1) The optimization process should make the ratio become larger. So the objective function was set as the following.

$$F(p_j) = |z_d / z_m| \tag{5}$$

Here, p_j was the design variable which expressed the

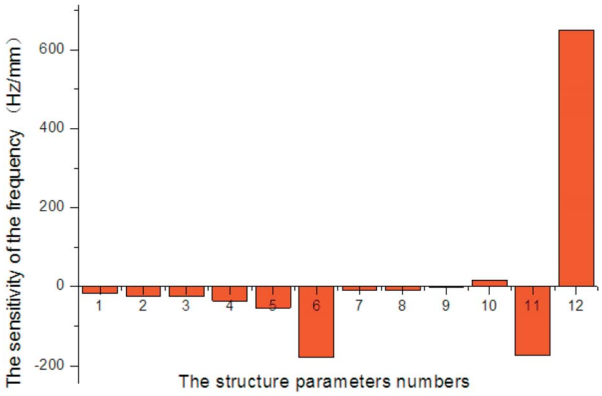

Figure 10. The sensitivity of the first order longitudinal frequency on the structure parameter.

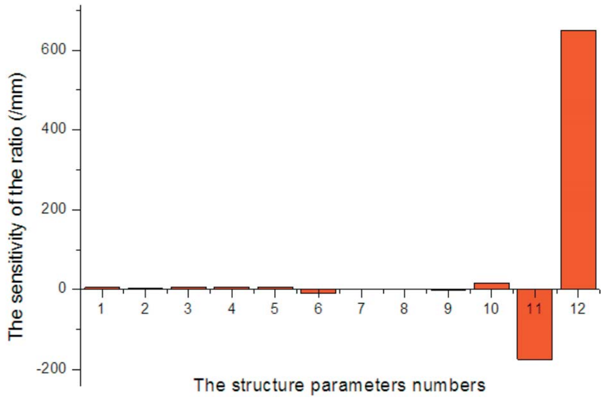

Figure 11. The sensitivity of the ratio on the structure parameter.

structure parameter of the ultrasonic vibrator. Depending on the result of the sensitivity, the structure parameters of L_5, L_6, Φ_5, Φ_6 would be selected as the design variables. z_d and z_m were respectively the first order longitudinal mode displacements of the node *d* and *m* which were shown in Figure 4.

(2) The piezoelectric ceramic and the connecting disk should be placed on the node plane of the first order longitudinal mode. The state variable was set as the following:

$$M_1(p_j) = |z_{j1}| + |z_{j2}| \quad (6)$$

Here, z_{j1} and z_{j2} were respectively the first order longitudinal mode values of the node of *j*1 and *j*2 which were shown in Figure 4. The node of *j*1 and *j*2 were respectively located at the edge of the ceramic and the connecting disk. When the value of $M_1(p_j)$ was smaller, the positions of the ceramic and the connecting disk were closer to the node plane of the first order longitudinal mode.

(3) The ultrasonic vibrator should have proper first order longitudinal mode frequency. The state variable was set as the following:

$$M_2(p_j) = f_L \quad (7)$$

Here, f_L was the value of 20~30 kHz.

By using the finite element analysis software ANSYS parametric design language APDL, the automatic optimization program was designed. Block Lanczos mode extraction method was adopted in modal analysis. The first order longitudinal mode displacement cloud chart of the vibrator after optimization was shown in Figure 12. The first order longitudinal mode frequency of the optimized ultrasonic vibrator was about 21.63 Hz and the ratio was about 186.8 in Figure 12.

Comparing Figure 7 and Figure 12, the optimization results were shown in Table 3. From the optimization results, the optimized vibrator could meet the design requirements.

4. Fabrication and Test of the Ultrasonic Vibrator

4.1 The Impedance and Phase Test

According to the results of the theoretical results, the

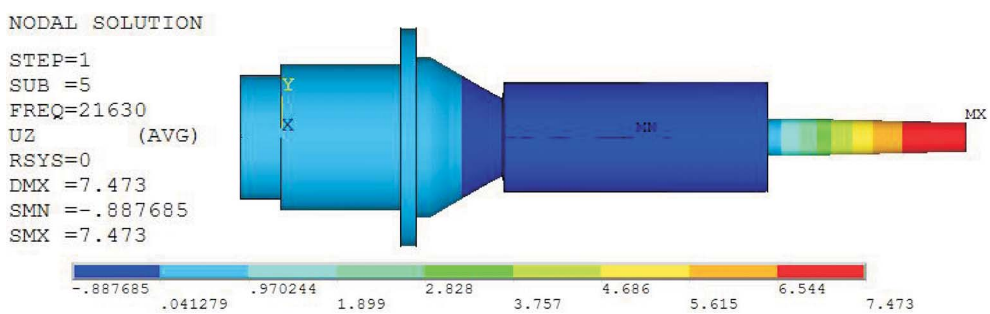

Figure 12. The axial displacement cloud chart of the first order longitudinal mode after optimization.

Table 3. The optimization results

	The parameters (mm)				$F(p_j)$	$M_1(p_j)$	$M_2(p_j)$
	L_5	L_6	Φ_5	Φ_6			
Before optimization	72	72	30	8	60.1	0.244	20.35
After optimization	70	70	32	6	186.8	0.04	21.63

ultrasonic vibrator was fabricated and assembled which were shown in Figure 13.

MODEL TH2818 series automatic component analyzer made by TONGHUI electronic company was used to test the impedance and phase of the ultrasonic vibrator which were shown shown in Figure 14.

The impedance and phase of the ultrasonic vibrator with 1 V excitation signal were shown in Figure 15. The frequency range of the excitation signal was 18–25 kHz. The test indicated that the resonant frequency was 21.747 kHz. The difference of the test result and the finite element calculation result (21.63 kHz) was approximately 0.54%.

4.2 The Modal Test of the Ultrasonic Vibrator

The modal of the ultrasonic vibrator was tested by using the laser Doppler vibrometer system PSV-300F-B made by Polytec Inc in Figure 16.

The sweep frequency chart of the ultrasonic vibrator was illustrated in Figure 17. The peak-peak value of the excitation voltage was 80 V and the sweep frequency range was approximately 18–26 Hz. In Figure 16 we could see the resonant frequency was about 21.45 kHz. The velocity of the front of the vibrator was approximately 580 mm/s at the frequency 21.45 kHz. Therefore the amplitude of the head was about 27 μm under the

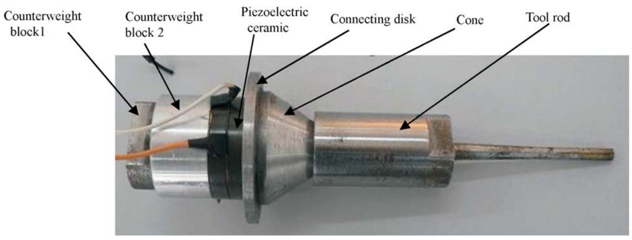

Figure 13. Photo of the ultrasonic vibrator.

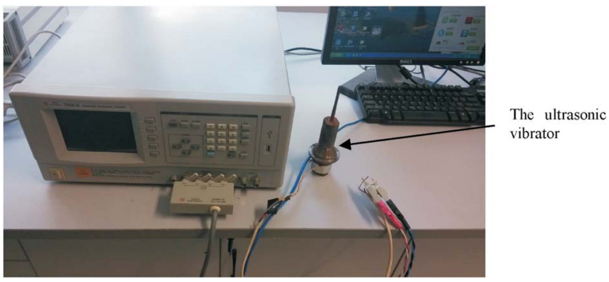

Figure 14. The impedance and phase test device.

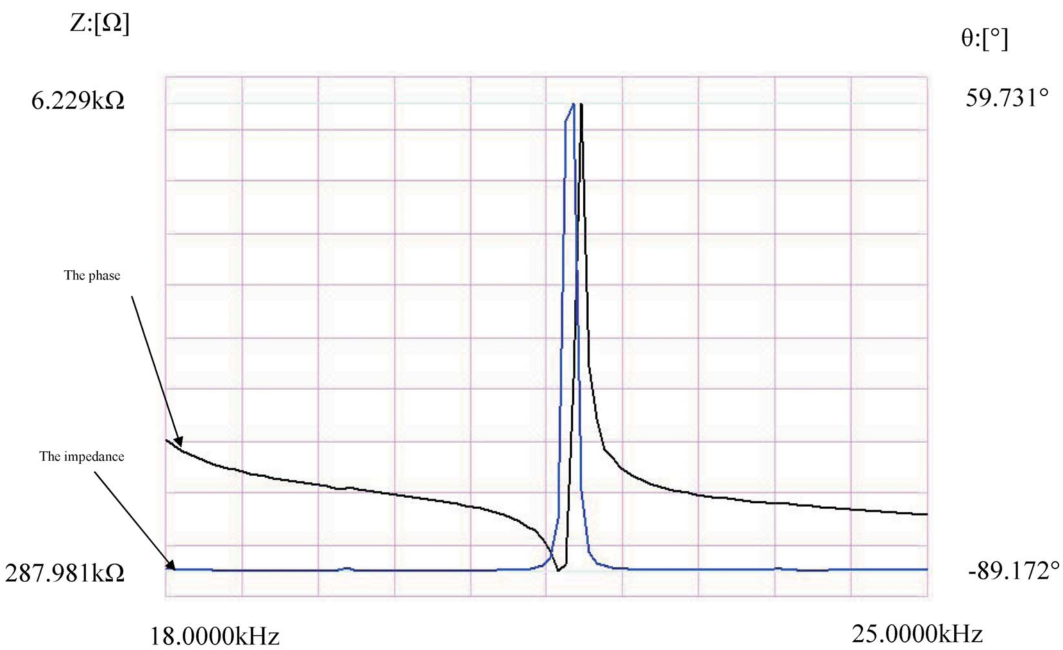

Figure 15. The impedance and phase of the ultrasonic vibrator.

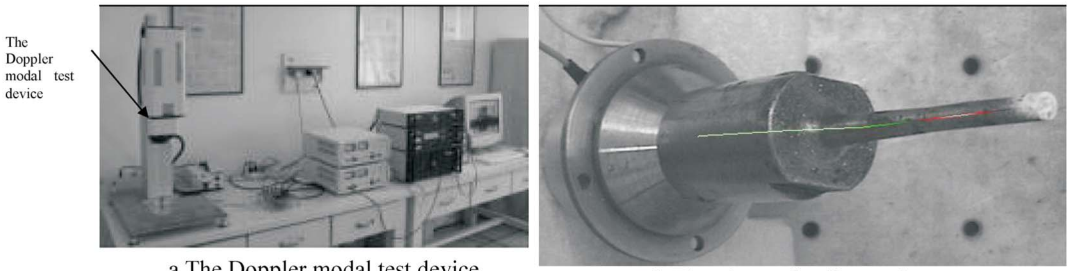

a The Doppler modal test device

b The ultrasonic vibrator for test

Figure 16. The Doppler modal test device and the ultrasonic vibrator for test.

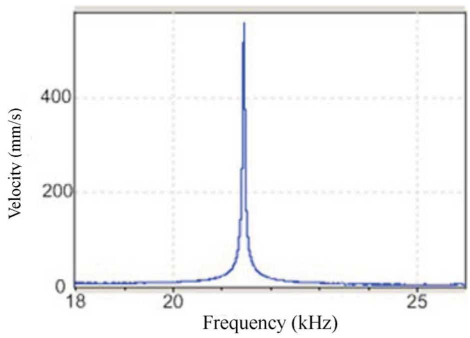

Figure 17. The sweep chart.

above conditions. The result was accorded with the results of the finite element calculation and the impedance test.

In Figure 18, the axial velocity distribution of the ultrasonic vibrator was applied to the same test conditions. The velocity of the front of the ultrasonic vibrator was maximum and decreased gradually along the axial direction. The result was according with the axial displacement cloud chart of the first order longitudinal mode in Figure 12. The frequency 21.45 kHz was the first order longitudinal mode frequency.

In Figure 18 we could also see the velocity of the head of the vibrator was about 580 mm/s and the velocity of the connecting disk was about zero. It met the desired requirements.

5. The Drilling Experiment

Hard and brittle materials including diorite, ceramic tile, limestone, granite, basalt, sandstone and glass were selected for drilling by using the drilling equipment. Seven materials were shown in Figure 19.

The peak-peak value of the working voltage was approximately 80 V and the working frequency was approximately 21.45 kHz. Emery and boron carbide mixed with water were respectively used as the working medium. The fineness of two abrasive was respectively 100 mesh and 240 mesh. Diorite, Ceramic tile, Limestone, Granite, Basalt, Sandstone and Glass were respectively numbered as 1, 2, 3, 4, 5, 6, 7. The drilling diameter was 3 mm with emery mixed with water used as the working

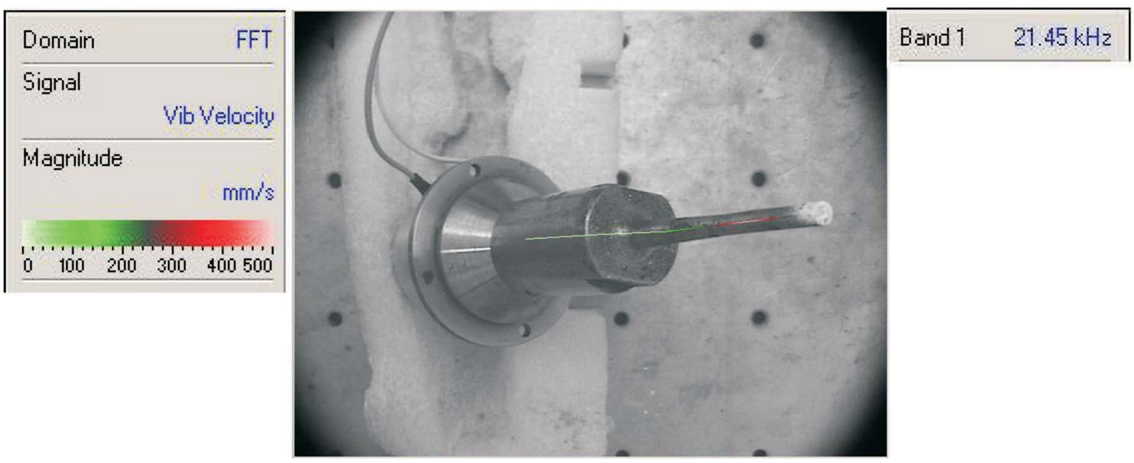

Figure 18. The velocity distribution test.

1-Diorite 2-Ceramic tile 3-Limestone 4-Granite
5-Basalt 6-Sandstone 7-Glass

Figure 19. The seven materials.

abrasive, and the drilling time was 1 min. The drilling depth of the seven materials was shown in Figure 20.

The drilling rate here was used to express the drilling efficiency and calculated by equation (8).

$$V = \frac{SH}{T} = \frac{\pi r^2 H}{T} (\text{mm}^3/\text{min}) \tag{8}$$

Here V was the drilling rate, H was the depth of the drilling hole, S was the area of the hole, r was the radius of the hole and T was the drilling time.

The drilling hole of Diorite velocity was calculated in equation (9) and was about 28.26 mm^3/min.

$$V = \frac{SH}{T} = \frac{\pi r^2}{T} = \frac{3.14 \times 1.5^2 \times 4}{1} = 28.26\ (\text{mm}^3/\text{min}) \tag{9}$$

The drilling rate was different with the fineness of the abrasive. For drilling the same material when the fineness of the abrasive was low the drilling rate was relatively fast.

The drilling quality was different with the different

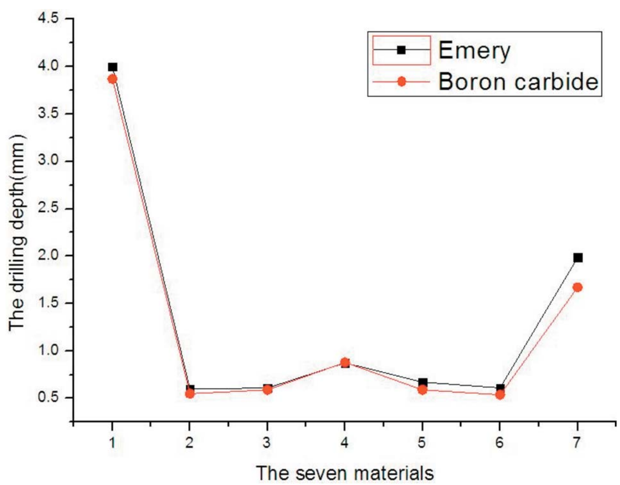

Figure 20. The drilling depth of the seven materials.

fineness of the abrasive. In Figure 21 two holes were respectively drilled on limestone and ceramic tile. The hole with a black circle was drilled using boron carbide whose fineness was 240 mesh (the grain size 61 μm) and the wall of the hole was smooth and neat. The quality of the hole was good. The other hole without black circle was drilled using emery whose fineness was 100 mesh (the grain size 150 μm). The wall of the hole was coarse.

From the result of the drilling experiment¡Ait was seen that the drilling device could drill effectively hard and crisp materials such as diorite, ceramic tile, limestone etc. With emery mixed with water used as the working abrasive, the rate of drilling diorite was about 28.26 mm^3/min.

6. Conclusion

The portable ultrasonic drilling equipment was designed and fabricated for drilling effectively hard and crisp materials such as diorite, ceramic tile, limestone etc. The ultrasonic vibrator was the main part of the ultrasonic drilling equipment. Through sensitivity analysis and optimization the ultrasonic vibrator was optimized to have proper first order longitudinal frequency, larger amplitude ratio, proper positions of the piezoelectric ceramic and the connecting disk. The first order longitudinal mode frequency was changed from 20.35 to 21.63 kHz and the ratio was changed from 60.1 to 186.8.

According to the theoretical analysis result, the ultrasonic vibrator was fabricated and assembled.The impedance, phase and modal test results of the ultrasonic vibrator were accorded with the theoretical results.

By the impedance and phase the resonant frequency was 21.747 kHz. The difference of the test result and the finite element calculation result (21.63 kHz) was about 0.54%.

The modal test results indicated that the velocity of

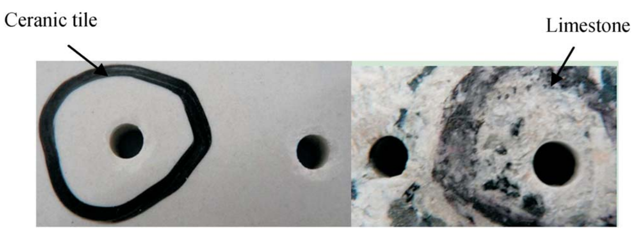

Figure 21. The drilling quality.

the vibrator's tip was the maximum, reached about 580 mm/s and the velocity of the vibrator's end was about 0.

The results of modal test were nearly accord with the results of the finite element calculation and the impedance test.

The drilling experiment could drill effectively hard and crisp materials such as diorite, ceramic tile, limestone etc. With emery mixed with water used as the working abrasive, the rate of drilling diorite diameter 3 mm was about 28.26 mm^3/min.

Acknowledgments

This work supported by the National Natural Science Foundation of China (51175359); Suzhou science and technology planning project (SYG201823); Sunzhou vocational university research project (SVU2018YY07, SVU2016CGCX12); sponsored by Qing Lan Project.

References

[1] Kang, I. S., J. S. Kim, et al. (2006)¡DA experimental study on the ultrasonic machining characteristics of engineering ceramics, *Journal of Mechanical Science and Technology* 20(2), 227–233. doi: 10.1007/BF 02915824

[2] Jeon, S. K., Y. J. Shin, B. H. Kim, H. Y. Kim, and B. H. Jeon (2003) Micro-machining of glass using chemical-assisted ultrasonic machining, *Transactions of KSME* 27(12), 2085–2091.

[3] Azarhoushang, B., and J. Akbari (2007) Ultrasonic-assisted drilling of Inconel 738-LC, *Intemational Journal of Machine Tools & Manufacture* 47(7–8), 1027–1033. doi: 10.1016/j.ijmachtools.2006.10.007

[4] Heisel, U., J. Wallaschek, R. Eisseler, et al. (2008) Ultrasonic deep hole drilling in electrolytic copper ECu 57, *CIRP Annals-Manufacturing Technology* 57(1), 53–56. doi: 10.1016/j.cirp.2008.03.078

[5] Liao, Y. S., Y. C. Chen, H. M. Lin, et. al. (2007) Feasibility study of the ultrasonic vibration assisted drilling of Inconel superalloy, *International Journal of Machine Tools & Manufacture* 47(12–13), 1988–1996. doi: 10.1016/j.ijmachtools.2007.02.001

[6] Kang, I. S., J. S. Kim, Y. W. Seo, and J. H. Kim (2006) An experimental study on the ultrasonic machining characteristics of engineering ceramics, *Journal of Mechanical Science and Technology* 20(2), 227–233. doi: 10.1007/BF02915824

[7] Wang, D. A., W. Y. Chuang, K. Hsu, et al. (2011) Design of a Bezier-profile horn for high displacement amplification, *Ultrasonics* 51(2), 148–156. doi: 10. 1016/j.ultras.2010.07.004

[8] Li, T., J. Ma, and A. F. Low (2011) Horn-type piezoelectric ultrasonic transducer: modelling and applications, Advances in Piezoelectric Transducers, Farzad Ebrahimi, Intech Open, 3–24. doi: 10.5772/28753

[9] Wang, H. B., Y. P. Zhang, Z. R. Li, and C. H. Sun (2014) A V-shaped small linear ultrasonic motor with multilayered piezoelectric stacks, *Indian Journal of Engineering and Materials Sciences* 21(5), 495–500.

Manuscript Received: Apr. 9, 2018
Accepted: Mar. 20, 2019